

## Original Article

# Generation of canine induced pluripotent stem cell-derived mesenchymal stem cells: Comparison of differentiation strategies and cell origins

Masaya Tsukamoto<sup>a</sup>, Chiaki Kawabata<sup>a</sup>, Kohei Shishida<sup>a</sup>, Takumi Yoshida<sup>a</sup>,  
Kazuto Kimura<sup>a,b</sup>, Kazuya Edamura<sup>c</sup>, Kikuya Sugiura<sup>a</sup>, Shingo Hatoya<sup>a,\*</sup>

<sup>a</sup> Department of Advanced Pathobiology, Graduate School of Veterinary Science, Osaka Metropolitan University, Izumisano, Osaka 598-8531, Japan

<sup>b</sup> Department of Pathology, Microbiology & Immunology, School of Veterinary Medicine, University of California, Davis, CA, USA

<sup>c</sup> Laboratory of Veterinary Surgery, Department of Veterinary Medicine, College of Bioresource and Sciences, Nihon University, Fujisawa, Kanagawa 252-0880, Japan

## ARTICLE INFO

## Article history:

Received 18 November 2023

Received in revised form

26 April 2025

Accepted 15 May 2025

## Keywords:

Canine

Induced pluripotent stem cell

Mesenchymal stem cell

Neural crest cell

Veterinary regenerative medicine

## ABSTRACT

**Introduction:** Mesenchymal stem cells (MSCs) possess immunomodulatory potential and are used for cell therapy in both human and veterinary medicine. However, donor-derived MSCs have limited proliferative activities and variations, which restrict their clinical applicability. In contrast, induced pluripotent stem cells (iPSCs) can self-renew indefinitely and differentiate into the three germ layers. By exploiting these characteristics, iPSCs can differentiate into mesenchymal stem cells (iMSCs) and potentially overcome the limitations of donor-derived MSCs. In humans, the characteristics of iMSCs have been reported to vary depending on the differentiation strategy and cell origin of iPSCs. However, no studies have investigated the differentiation strategies and cell origins of canine iPSCs (ciPSCs) in relation to iMSC generation.

**Methods:** Canine embryonic fibroblast-derived iPSCs (CEF-iPSCs) were differentiated into iMSCs via the mesoderm or ectoderm, and their proliferative ability and the expression levels of CD34, CD44, CD45, and CD90 were assessed. We then applied the iMSC induction method via the ectoderm to other ciPSC lines, including canine dermal fibroblast-derived iPSCs (CDF-iPSCs), canine peripheral mononuclear cell-derived iPSCs (cPBMC-iPSCs), and canine urine-derived cell-derived iPSCs (cUC-iPSCs). We assessed their proliferation, marker expression, and ability to differentiate into tri-lineages and performed comparative analyses.

**Results:** iMSCs derived from CEF-iPSCs via the ectodermal lineage showed higher proliferative ability and expressed MSC markers at a higher rate than iMSCs generated via mesodermal induction. Notably, with the exception of CDF-iPSCs, iMSCs were successfully generated from other ciPSC lines via ectodermal lineages. These iMSCs exhibited proliferative activities over passage 10, expressed MSC markers, and demonstrated the ability to differentiate into tri-lineages. iMSCs derived from cUC-iPSCs exhibited the highest expression of CD90 compared to other iMSCs.

**Conclusions:** Highly proliferative iMSCs expressing a high rate of MSC markers can be obtained from cUC-iPSCs via ectodermal induction. Our study demonstrated that the differentiation strategy and cell origin of ciPSCs play crucial roles in the generation of iMSCs.

© 2025 The Author(s). Published by Elsevier BV on behalf of The Japanese Society for Regenerative Medicine. This is an open access article under the CC BY-NC-ND license (<http://creativecommons.org/licenses/by-nc-nd/4.0/>).

**Abbreviations:** iPSCs, induced pluripotent stem cells; iMSCs, iPSC-derived mesenchymal stem cells; MSCs, mesenchymal stem cells; LPM, lateral plate mesoderm; NCCs, neural crest cells; ciPSCs, canine induced pluripotent stem cells; CEFs, canine embryonic fibroblasts; CDFs, canine dermal fibroblasts; cPBMCs, canine peripheral mononuclear cells; cUCs, canine urine-derived cells; KSR, knockout serum replacement; FBS, fetal bovine serum.

This article is part of a special issue entitled: Future of Regenerative Medicine published in Regenerative Therapy.

\* Corresponding author.

E-mail address: [hatoya@omu.ac.jp](mailto:hatoya@omu.ac.jp) (S. Hatoya).

Peer review under responsibility of the Japanese Society for Regenerative Medicine.

<https://doi.org/10.1016/j.reth.2025.05.008>

2352-3204/© 2025 The Author(s). Published by Elsevier BV on behalf of The Japanese Society for Regenerative Medicine. This is an open access article under the CC BY-NC-ND license (<http://creativecommons.org/licenses/by-nc-nd/4.0/>).

## 1. Introduction

Human mesenchymal stem cells (MSCs) are plastically adherent cells derived from various tissues that express surface markers, including CD73, CD90, and CD105, but lack the expression of hematopoietic and endothelial markers. MSCs can differentiate into adipocytes, chondrocytes, and osteoblasts [1,2]. Owing to their immunomodulatory effects, MSCs have been used in various clinical trials in the fields of cardiology, pulmonology, and the immunomodulation of immune diseases [3]. Canines naturally develop diseases similar to humans, and canine MSCs have been shown to have immunomodulatory effects similar to human MSCs [4–6]. Therefore, canine MSCs have also been used in veterinary regenerative medicine [7].

Despite the wide application of MSCs in cell-based therapies in human and veterinary medicine, their clinical utility remains limited [8]. This limitation arises from the restricted proliferation capabilities and variations shown by donor-derived MSCs, which are influenced by factors such as donors, passage numbers, and culture conditions [9–12]; these variabilities are the major barrier for good clinical usefulness.

Pluripotent stem cells (PSCs), including embryonic stem cells and induced pluripotent stem cells (iPSCs), have the remarkable ability to self-renew indefinitely and differentiate into all three germ layers. Leveraging these characteristics, MSC generation from iPSCs offers a potential solution to overcome the limitations associated with donor-derived MSCs [8,13]. Numerous studies have reported the generation of MSCs from human PSCs [14,15]. MSCs induced from iPSC (iMSCs) derivation protocols can be broadly categorized into two groups based on their cell origins. One approach involves direct mesodermal induction by targeting the lateral plate mesoderm (LPM). Another approach involves induction of iMSCs through the ectoderm, specifically through neural crest cells (NCCs). Importantly, a study has reported that iMSCs derived from these two protocols show distinct characteristics [16]. Although there have been reports of iMSC induction from canine iPSCs (ciPSCs) [17,18], no investigation has been conducted to determine whether LPM or NCCs can generate high-quality iMSCs from ciPSCs. Furthermore, although human iPSC lines exhibit variations in their ability to differentiate into specific lineages owing to epigenetic memory inherited from somatic cells or de novo variations during cell reprogramming and extended culture [19], there is no evidence that such variations exist in ciPSCs.

Therefore, it is important to efficiently generate high-quality iMSCs from ciPSCs for transplantation. We hypothesized that the differentiation protocol and ciPSC variability influence the differentiation kinetics and quality of canine iMSCs. To test this hypothesis and provide valuable insights for veterinary regenerative medicine, we compared the two iMSC induction protocols, via LPM and NCCs, using canine embryonic fibroblast (CEF) derived iPSCs (CEF-iPSCs). Furthermore, we investigated the influence of ciPSC variability on the differentiation kinetics and iMSC features using ciPSC lines generated from other cell origins. Our findings will facilitate future studies using iMSCs derived from ciPSCs in veterinary regenerative medicine.

## 2. Materials and methods

### 2.1. ciPSC culture

CEF-iPSCs (OPUiEF1-D-2), canine dermal fibroblast (CDF) derived iPSCs (CDF-iPSCs) (OPUiD05-FA-1), and canine urine-derived cell (cUC) derived iPSCs (cUC-iPSCs) (OPUiD02-UD-1) were established using Sendai virus (SeV) encoding canine KLF4,

OCT3/4, SOX2, C-MYC, LIN28A, and NANOG [20]. cPBMC-iPSCs (OPUiD04-B) were generated using SeV encoding human KLF4, OCT3/4, SOX2, and C-MYC [21]. They were maintained using a laminin-511-E8 fragment (iMatrix511; Nippi, Tokyo, Japan) and StemFit AK02 N (StemFit; Ajinomoto, Tokyo, Japan) at 37 °C and 5 % CO<sub>2</sub> and passaged mechanically using a Pasteur pipet every 5 or 6 days.

### 2.2. iMSC induction via LPM

The iMSCs were derived according to a previous study with some modifications [22], as illustrated in Fig. 1A. Briefly, ciPSCs were plated as cell clusters on Matrigel-coated dishes (Corning Inc., Corning, NY, USA). After 2–5 days, the medium was changed to KSR + SB medium, which consisted of Dulbecco's Modified Eagle Medium/Nutrient Mixture F-12 Ham (DMEM/F-12; Nacalai Tesque, Kyoto, Japan) with 20 % knockout serum replacement (KSR; Thermo Fisher Scientific, Waltham, MA, USA), 2 mM L-glutamine (Nacalai Tesque), 100 IU/mL penicillin, 100 µg/mL streptomycin (Nacalai Tesque), 0.1 mM non-essential amino acid (Nacalai Tesque), 0.1 mM 2-mercaptoethanol (Thermo Fisher Scientific), and 10 µM transforming growth factor β (TGFβ) inhibitor (SB431542; Fujifilm Wako Pure Chemical Corporation, Osaka, Japan). After 10 days, the cells were dissociated using the TrypLE Select Enzyme (Thermo Fisher Scientific) and seeded into tissue culture dishes at a density of  $4.0 \times 10^4/\text{cm}^2$ . They were cultured in fetal bovine serum (FBS)-containing MSC medium (FBS-MSC medium), which consisted of Minimum Essential Medium α with 2 mM GlutaMAX (Thermo Fisher Scientific), 10 % FBS (Sigma-Aldrich, St. Louis, MO, USA), 100 IU/mL penicillin, 100 µg/mL streptomycin, 10 ng/mL basic fibroblasts growth factor (bFGF; Peprotech, Rocky Hill, NJ, USA) at 37 °C and 5 % CO<sub>2</sub>. The FBS-MSC medium was replaced every other day and bFGF was added daily. For subsequent passages, the cells were seeded at a density of  $2.0 \times 10^4/\text{cm}^2$ .

### 2.3. iMSC induction via NCCs

The iMSCs were induced via NCCs following a previously described protocol [23] with some modifications (Fig. 1B and C). Briefly, 3–5 days after passage, ciPSCs were cultured in NCC induction medium, which consisted of StemFit without supplement C (StemFit without C) supplemented with 10 ng/mL bFGF, 10 µM SB431542, 1 µM glycogen synthase kinase 3β (GSK3β) inhibitor (CHIR99021; Fujifilm Wako Pure Chemical Corporation) for 10 days at 37 °C and 5 % CO<sub>2</sub>. The cells were then collected using TrypLE Select Enzyme, seeded onto a fibronectin (Sigma-Aldrich)-coated dish at a density of  $2.0 \times 10^4$ – $1.2 \times 10^5$  cells/cm<sup>2</sup>, and cultured in NCC maintenance medium, which consisted of StemFit without C supplemented with 20 ng/mL bFGF, 10 µM SB431542, and 20 ng/mL human epidermal growth factor (EGF; Thermo Fisher Scientific). The medium was changed daily. After several passages, when the NCCs reached approximately 50 % confluence, they were cultured in either StemFit for mesenchymal stem cells (Ajinomoto) (referred to as NCC + StemFit) or PRIME-XV MSC expansion XFSM (Fujifilm Wako Pure Chemical Corporation) (referred to as NCC + PRIME). In the NCC + StemFit protocol, the cells were maintained on iMatrix511, while in the NCC + PRIME protocol, the cells were cultured on fibronectin. The medium was changed every 2 or 3 days.

### 2.4. Evaluation of iMSC characteristics

#### 2.4.1. Cell doubling time

iMSCs derived using each protocol were counted at each passage. Cell doubling time was calculated as follows.

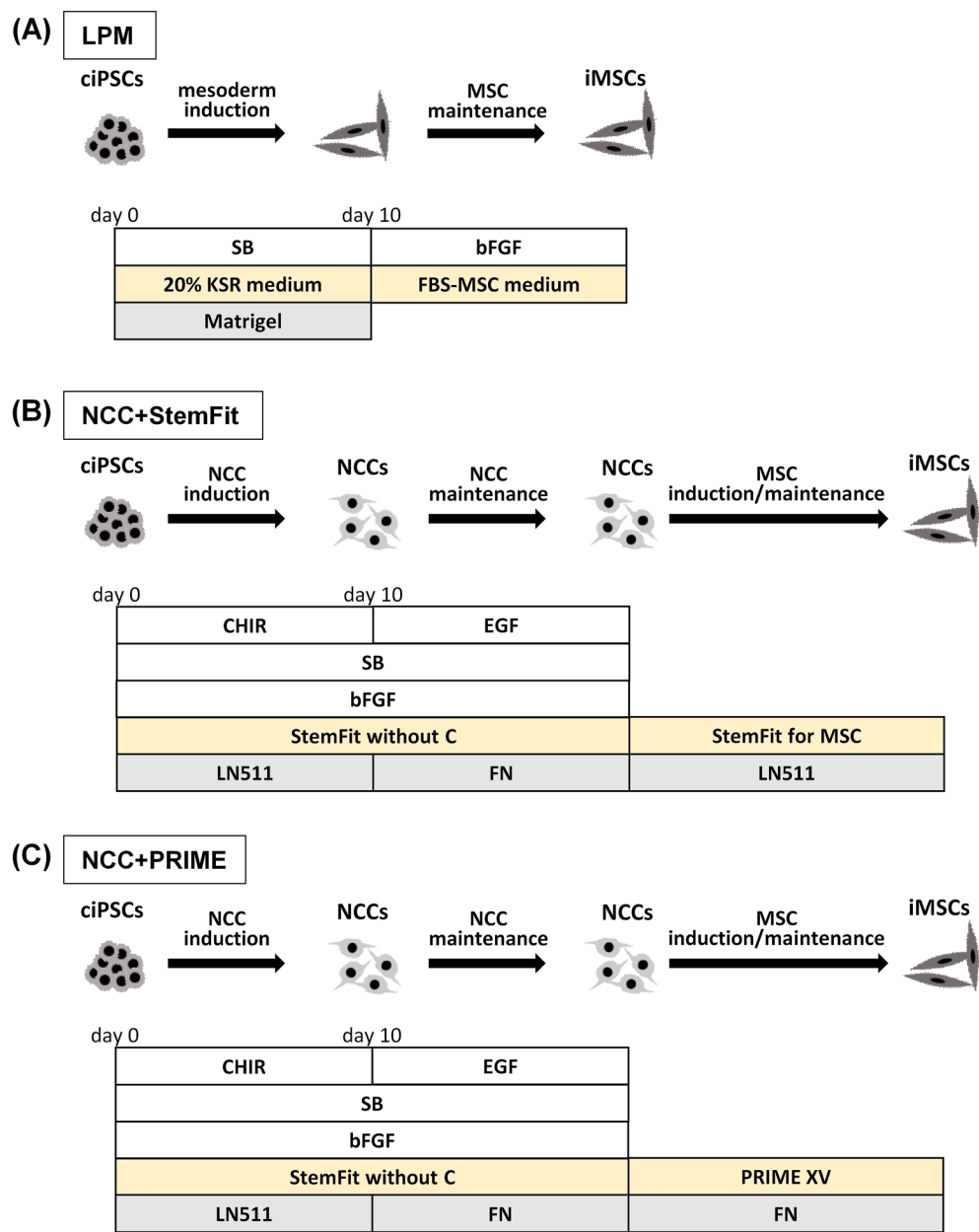


**Fig. 1.** Schema to obtain induced pluripotent stem cell (iPSC)-derived mesenchymal stem cells (iMSCs). (A) A method for iMSC generation via lateral plate mesoderm (LPM). To induce mesodermal lineage, canine iPSCs (ciPSCs) were cultured on Matrigel with 20 % knockout serum replacement (KSR) medium containing transforming growth factor  $\beta$  (TGF $\beta$ ) signal inhibitor, SB431542 (SB). After passages, the cells were cultured on tissue-culture dishes with fetal bovine serum (FBS)-MSC medium containing basic fibroblast growth factor (bFGF). We described this iMSC induction protocol as the LPM protocol. (B) A method for iMSC generation via neural crest cells (NCCs). To induce NCCs, ciPSCs were cultured with laminine-511 (LN511) and StemFit without solution C (StemFit without C) containing glycogen synthetase kinase 3 $\beta$  (GSK3 $\beta$ ) inhibitor, CHIR99031 (CHIR), SB, and bFGF. After neural specification, the cells were maintained in NCC maintenance medium, which was StemFit without C containing SB, bFGF, and epidermal growth factor (EGF) on fibronectin (FN). When NCCs differentiated into iMSCs, they were cultured with StemFit for mesenchymal stem cells and LN511. We described this iMSC induction protocol as NCC + StemFit. (C) iMSC induction method via NCCs using other iMSC culture conditions. NCCs generated as described in (B) were induced to iMSCs by culturing with PRIME-XV MSC expansion XFSM on FN. We described this iMSC induction protocol as NCC + PRIME.

Doubling time = culture time (day)  $\times$  log2/(logNt-logN0).  
Nt: the harvested cell number after culture, N0: the starting cell number.

**2.4.2. Analysis of cell surface antigens using flow cytometry**  
iMSCs at each passage were dissociated using 0.25 % trypsin-EDTA (Sigma-Aldrich). Cell pellets were resuspended in FACS buffer consisting of phosphate-buffered saline (PBS) (–) (Nacalai Tesque) containing 2 % FBS and 1 mg/mL sodium azide (Fujifilm Wako Pure Chemical Corporation). The cells were then labeled with

specific antibodies on ice for 30 min. Negative control cells were incubated with the appropriate isotype control. Subsequently, the cells were washed with FACS buffer and analyzed using a flow cytometer (CytoFLEX, Beckman Coulter, CA, USA). The antibodies used in this study are listed in the [Supplementary Table 1](#).

**2.4.3. Osteoblast induction from iMSCs**  
iMSCs were seeded onto a fibronectin-coated dish at a density of  $2.0 \times 10^4$ /cm<sup>2</sup>. The cells were cultured in canine osteoblast differentiation medium (Cell Applications, San Diego, CA, USA) for 28

days at 37 °C and 5 % CO<sub>2</sub>. The medium was changed every 3 days. Differentiation into osteoblasts was assessed using quantitative RT-PCR (qPCR) or Von Kossa staining. For staining, the cells were fixed in 96 % ethanol (Nacalai Tesque) for 15 min and washed with pure water. Subsequently, the cells were treated with 5 % silver nitrate (Fujifilm Wako Pure Chemical Corporation) at 25 °C for 1 h under light exposure. After washing with pure water, the cells were treated with 5 % sodium thiosulfate (Fujifilm Wako Pure Chemical Corporation) for 3 min and washed again with pure water.

#### 2.4.4. Adipocyte induction from iMSCs

iMSCs were seeded onto a Geltrex (Thermo Fisher Scientific)-coated dish at a density of  $2.0 \times 10^4/\text{cm}^2$ . The cells were cultured in canine adipocyte differentiation medium (Cell Applications) for 21 days at 37 °C and 5 % CO<sub>2</sub>. The medium was changed every other day. Differentiation into adipocytes was assessed using qPCR or Oil Red O staining. Briefly, the cells were washed with PBS (–) and fixed in 4 % paraformaldehyde (PFA) for 5 min. After washing with PBS (–), the cells were treated with 60 % 2-propanol (Nacalai Tesque). The cells were then stained with 0.18 % Oil Red O (Fujifilm Wako Pure Chemical Corporation) for 15 min in the dark. Subsequently, the cells were treated with 60 % 2-propanol and washed twice with PBS (–).

#### 2.4.5. Chondrocyte induction from iMSCs

iMSCs were seeded into a 96 well U bottom plate (Thermo Fisher Scientific) at a density of  $5.0 \times 10^5/\text{well}$ . The cells were then cultured in canine chondrocyte differentiation medium (Cell Applications) for 30 days at 37 °C and 5 % CO<sub>2</sub>. The medium was changed every day. Differentiation into chondrocytes was assessed using qPCR or Alcian blue staining. For staining, cell spheres were fixed in 4 % PFA and embedded in paraffin. Sections of the spheres were treated with 3 % acetic acid for 3 min, stained with 1 % Alcian blue (Fujifilm Wako Pure Chemical Corporation) for 30 min, and rinsed with water. Subsequently, the sections were stained with 0.1 % Nuclear Fast Red (Tokyo Chemical Industry Co., Tokyo, Japan) for 5 min and washed with water for 3 min. Finally, the sections were dehydrated in ethanol and xylene for 5 min and mounted using MGK-S (Matsunami Glass, Osaka, Japan).

#### 2.4.6. Quantitative RT-PCR

Total RNA was extracted using the FastGene™ RNA Premium Kit (Nippon Genetics, Tokyo, Japan). Reverse transcription (RT) was performed using random primers and ReverTra Ace (Toyobo, Osaka, Japan). Polymerase chain reaction (PCR) was performed using THUNDERBIRD Next SYBR™ qPCR Mix (Toyobo) and a StepOnePlus real-time PCR machine (Thermo Fisher Scientific).  $\beta$ -ACTIN was used as a normalization control gene, and relative gene expression levels were calculated by  $\Delta\Delta\text{Ct}$  method. All primers are listed in [Supplementary Table 2](#).

### 2.5. Statistical analysis

Data are expressed as the mean  $\pm$  standard deviation. Statistical significance was determined using Tukey–Kramer multiple comparison or Student's t-test using Statcel software (OMS Ltd., Tokorozawa, Japan).

## 3. Results

### 3.1. iMSC generation and characterization from CEF-iPSCs via LPM and NCCs

After cultivating CEF-iPSCs in KSR + SB medium, a morphological change from epithelial to spindle shape was observed

([Fig. 2A](#)). These cells maintained their spindle morphology throughout the passages in the FBS-MSC medium ([Fig. 2A](#)). In contrast, when CEF-iPSCs were differentiated using NCC induction medium, iPSC colonies became dome-shaped, and some cells differentiated into neuron-like cells ([Fig. 2B](#)). Subculturing and maintenance of these cells in NCC maintenance medium resulted in cells acquiring an NCC-like dendritic morphology ([Fig. 2B](#)). These cells expressed the neural progenitor markers NESTIN, SOX2, and PAX6 but did not express the pluripotent marker OCT3/4 or the neuronal marker TUBB3 ([Fig. 2C](#) and [Supplementary Fig. 1](#)). Following culture in StemFit for mesenchymal stem cells or PRIME-XV MSC expansion in XSFM, morphological changes were observed, and spindle-shaped cells proliferated ([Fig. 2D](#) and [E](#)).

iMSCs using the LPM protocol (LPM-iMSCs) maintained their morphologies until passage three, but after several passages, they exhibited swelling and ceased proliferation, as indicated by their increased doubling time until passage five ( $n = 3$ ) ([Fig. 3A](#)). iMSCs derived from NCC + StemFit (StemFit-iMSCs) initially displayed spindle morphology but lost their MSC-like characteristics by passage three. Their growth was limited and ceased by passage eight ([Fig. 3A](#)). In contrast, iMSCs derived using NCC + PRIME (PRIME-iMSCs) maintained their spindle morphology, continued to proliferate, and retained their phenotype until passage 13 ([Fig. 3A](#)). Comparative marker expression analysis of LPM-, StemFit-, and PRIME-iMSCs using flow cytometry revealed that PRIME-iMSCs exhibited higher expression of CD90 and CD44 than StemFit-iMSCs ([Fig. 3B](#)). None of the LPM-, StemFit-, or PRIME-iMSCs expressed the MSC markers CD34 and CD45 ([Fig. 3B](#)).

Based on these results, it was confirmed that the NCC + PRIME protocol successfully generated iMSCs, that had the highest proliferative capacity and expressed MSC-positive markers at the highest rate.

### 3.2. PRIME-iMSCs could be generated from other ciPSC lines

Next, we generated PRIME-iMSCs from different iPSC sources, including CDF-iPSCs, cUC-iPSCs, and cPBMC-iPSCs. All ciPSC lines formed three-dimensional colonies when cultured in the NCC induction medium ([Fig. 4A](#)). In line with the findings for CEF-iPSCs, it was also observed that some cells derived from cUC-iPSCs and cPBMC-iPSCs differentiated into neuron-like cells. Moreover, these cells could be maintained in the NCC maintenance medium. They expressed SOX2, NESTIN, and PAX6, but not OCT3/4 or TUBB3 ([Supplementary Figs. 2 and 3](#)). However, the cells that differentiated from CDF-iPSCs did not proliferate in NCC maintenance medium and appeared to differentiate into neuron-like cells with round cell bodies and elongated axon-like structures ([Fig. 4A](#)). MSC-like cells were obtained after culturing NCCs from cUC-iPSCs and cPBMC-iPSCs in PRIME-XV MSC expansion XSFM ([Fig. 4A](#)). The PRIME-iMSCs derived from CEF-, cUC-, and cPBMC-iPSCs maintained their proliferative activity and exhibited bipolar or multipolar shapes over multiple passages ([Fig. 4B](#)).

Marker expression analysis of PRIME-iMSCs from different iPSC sources revealed that all PRIME-iMSCs expressed CD44 at a rate similar to that of the adipose-derived MSCs Ad-MSCs ([Fig. 5](#)). The expression of CD90 varied among different iPSC sources. Notably, PRIME-iMSCs from cUC-iPSCs exhibited an increasing proportion of CD90-positive cells over subsequent passages, reaching approximately 90 % by passage seven. However, PRIME-iMSCs from CEF- and cPBMC-iPSCs expressed at a lower rate than Ad-MSCs, even after multiple passages ([Fig. 5](#)). All PRIME-iMSCs from the CEF-, cUC-, and cPBMC-iPSCs were negative for CD34, CD45, and SSEA1 ([Fig. 5](#)). qPCR analysis indicated a similar trend for CD90 expression as observed with flow cytometry



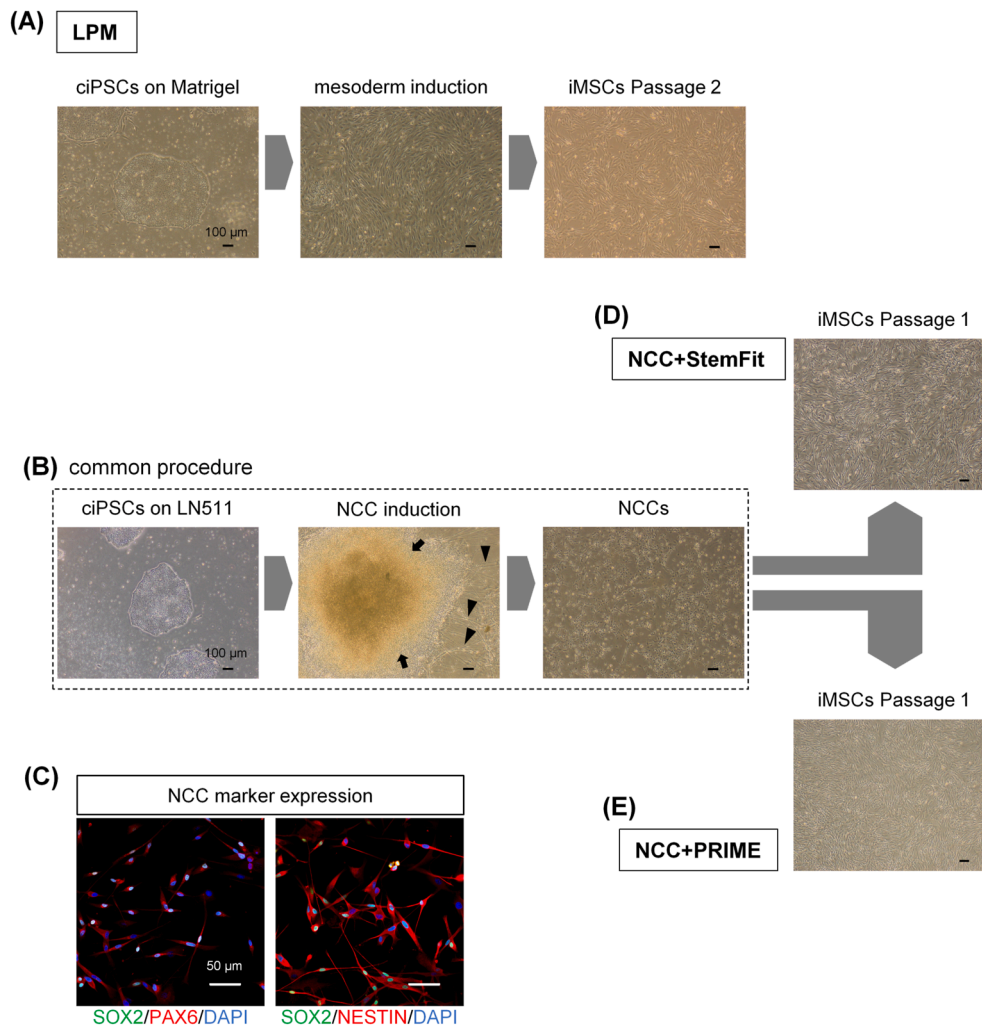


**Fig. 2.** Morphological changes during mesenchymal stem cell (MSC) induction from canine embryonic fibroblast (CEF)-derived induced pluripotent stem cells (iPSCs). (A) Cell morphologies with lateral plate mesoderm protocol. Before differentiation, canine iPSCs (ciPSCs) on Matrigel maintained their undifferentiated colony shapes. After approximately 8 days from mesoderm induction, the cells exhibited spindle shapes. iPSC-derived mesenchymal stem cells (iMSCs) maintained their spindle morphologies after several passages. Scale bar = 100  $\mu$ m. (B–E) Morphological changes during iMSC induction via neural crest cells (NCCs). (B) A common procedure for inducing NCCs from ciPSCs (squared with black dashed line). ciPSCs cultured on laminin-511 (LN511) had flat colony morphologies and became dome-shaped 10 days after NCC induction (black arrow). Some cells differentiated into neuron-like cells (black arrowheads). Subculturing and maintenance of these cells in NCC maintenance medium resulted in cells acquiring an NCC-like dendritic morphology. (C) NCC expression of the neural progenitor markers NESTIN, SOX2, and PAX6, as detected by immunocytochemistry. Scale bar = 50  $\mu$ m. (D) and (E) show the iMSC morphologies derived using the NCC + StemFit and NCC + PRIME protocols, respectively. Scale bar = 100  $\mu$ m.

(Supplementary Fig. 4). qPCR also showed that PRIME-iMSCs rarely express *CD105*, a positive marker for human and canine MSCs [1,6], or *CD74*, also known as HLA-DR in humans and corresponds to the canine invariant chain of the major group of histocompatibility class II (MHC-II) (Supplementary Fig. 4) [24].

Furthermore, the tri-lineage differentiation ability of PRIME-iMSCs was assessed. After osteoblast induction, all PRIME-iMSCs were positive for Von Kossa staining and upregulated osteoblast markers, *SPP1* and *BGLAP* (Fig. 6A). Following adipocyte induction, all PRIME-iMSCs differentiated into adipocytes, as confirmed by Oil Red O staining, although only a small portion of cells exhibited positive staining. qPCR revealed that *PLIN1* was induced in differentiated cells; however, statistical significance was not observed due to data variability (Fig. 6B). Similarly, after chondrocyte induction, all PRIME-iMSCs formed spheres and stained positive for Alcian blue, and chondrocyte-induced cells expressed *ACAN* and *SOX9* (Fig. 6C).

#### 4. Discussion

To obtain iMSCs from ciPSCs, we first differentiated CEF-iPSCs into iMSCs using two different protocols, via LPM or NCCs, and compared their characteristics. Our findings demonstrated that iMSCs derived from NCCs in PRIME-XV medium exhibited the highest proliferative ability and expressed MSC-positive markers at the highest rate. Although human iMSCs have been reported to exhibit greater proliferative capacity and telomerase activity than those derived from tissue-derived MSCs [25], this does not apply to canine cells due to the limited proliferative potential of LPM-iMSCs. One possible explanation is that PRIME-iMSCs were cultured in PRIME-XV serum-free medium. Higher proliferation activities in serum-free medium have also been reported in human [26] and canine MSCs [27], as well as human iMSCs [28]. Another reason for the success of NCC + PRIME method may be that iMSCs were derived via NCCs rather than direct mesodermal induction.

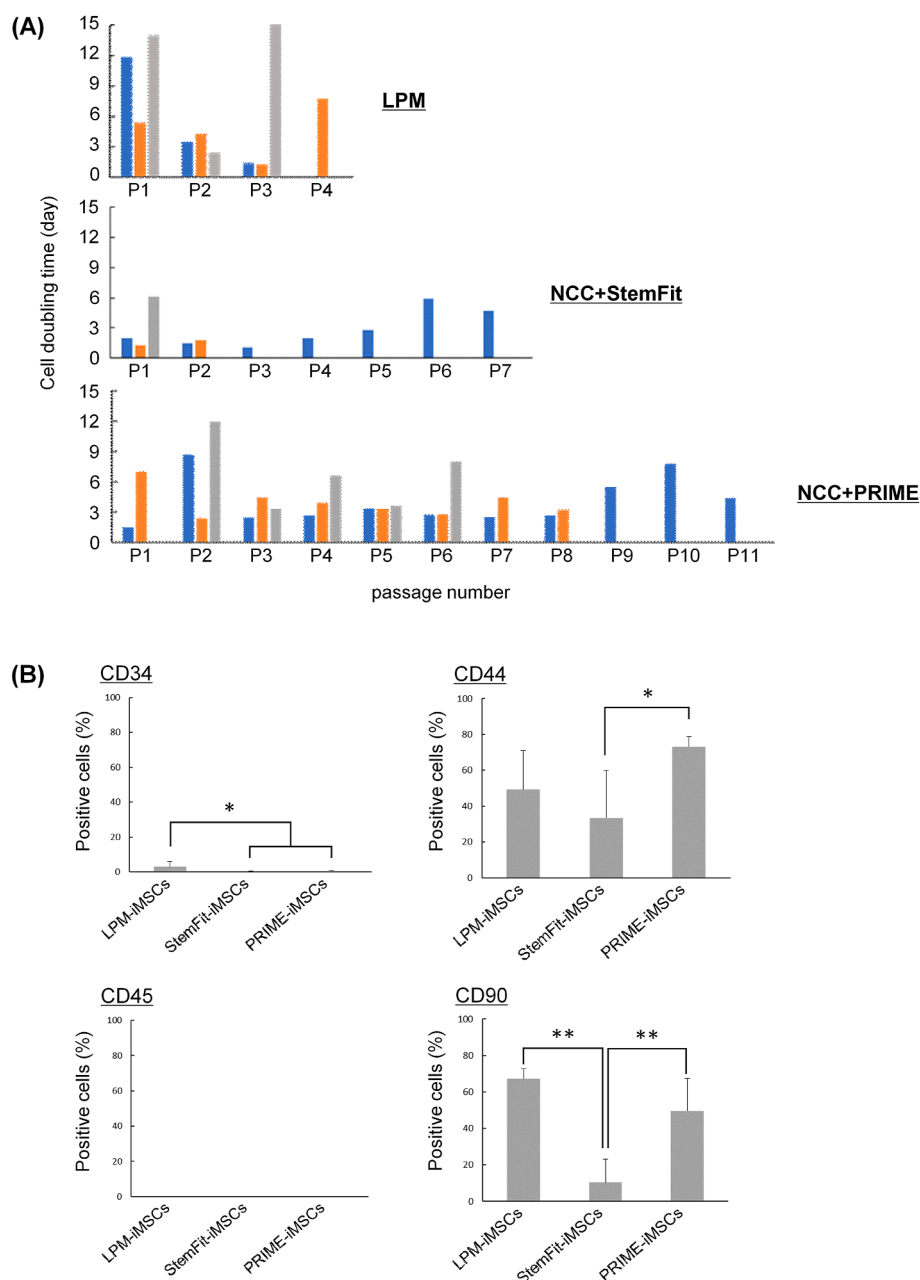


**Fig. 3.** Induced pluripotent stem cell-derived mesenchymal stem cells (iMSCs) proliferative activities and marker expression. (A) Cell doubling time of iMSCs generated by three protocols, lateral plate mesoderm (LPM), neural crest cells (NCC) + StemFit, and NCC + PRIME at each passage number. Each bar color indicates a biological replicate. (B) Flow cytometry analysis of iMSCs generated by three methods for hematopoietic markers CD34 and CD45, and mesenchymal markers CD44 and CD90 at passage number 1. Each experiment was performed three times as biological replicates. Data are shown as the mean  $\pm$  standard deviation ( $n = 3$ ). Asterisks indicate statistical significance: \* $p < 0.05$ , \*\* $p < 0.01$ . LPM-iMSCs, StemFit-iMSCs, and PRIME-iMSCs represent iMSCs derived by the LPM, NCC + StemFit, and NCC + PRIME protocols, respectively.

The standardized protocol after several passages as NCCs might influence the results. However, it should be noted that another serum-free medium, StemFit-iMSCs, could not maintain their MSC characteristics from NCCs. This supports the hypothesis that culture conditions play a pivotal role in the quality of ciPSC-derived iMSCs. We concluded that the combination of the differentiation method (via NCCs) and expansion medium (serum-free medium, especially PRIME-XV MSC expansion XSFM) is optimal for producing highly proliferative iMSCs from CEF-ciPSCs, although we could not evaluate these two factors independently. This approach is beneficial to prepare a large number of cells for cell therapy, despite not assessing karyotypes and tumorigenesis of iMSCs in this study.

We successfully generated PRIME-iMSCs from CEF-iPSCs, as well as cUC- and cPBMc-iPSCs. This indicated that the NCC + PRIME protocol was reproducible for iMSC generation from ciPSCs, and PRIME-iMSCs from three different cell lines fulfilled the minimum criteria for canine MSCs, including morphology, marker expression of CD44 and CD90, and tri-lineage differentiation ability [29], although there are no definitive marker expression criteria for canine tissue-derived MSCs, unlike those established for human MSCs [1,2]. Flow cytometry revealed that PRIME-iMSCs expressed CD44 at levels comparable to Ad-MSCs, while qPCR indicated that PRIME-iMSCs barely expressed *CD105*. Canine tissue-derived MSCs exhibit variable *CD105* expression depending on the tissue source and experimental conditions [30].

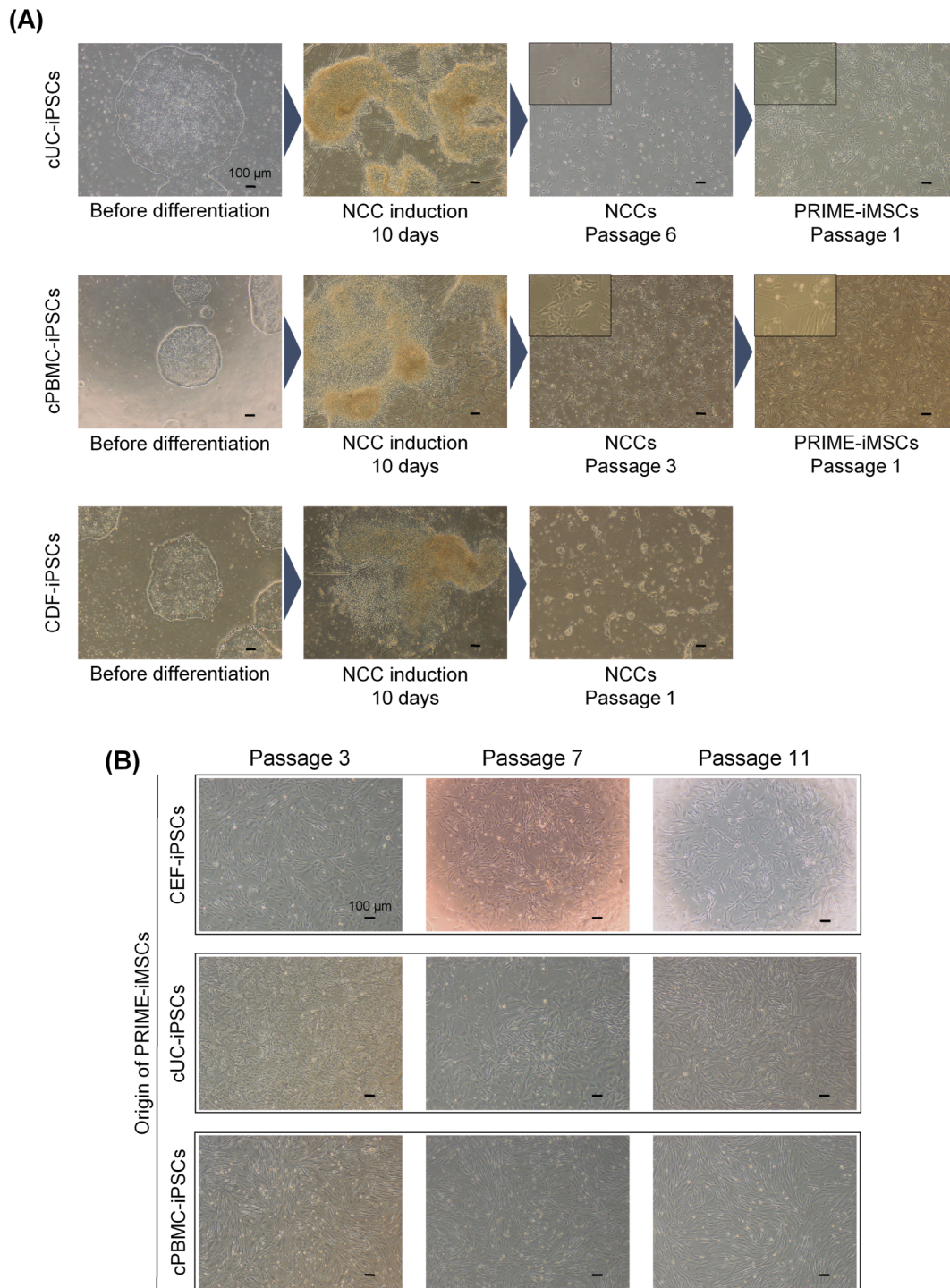


**Fig. 4.** Mesenchymal stem cell (MSC) induction from other canine induced pluripotent stem cell (ciPSC) lines originated from various tissues. (A) MSCs were induced using the neural crest cell (NCC) + PRIME protocol (PRIME-iMSCs). ciPSCs originated from canine urine-derived cells (cUCs), canine peripheral blood mononuclear cells (cPBMCs), or canine dermal fibroblasts (CDFs) were used. Morphological differences were not observed before differentiation and 10 days after NCC induction. NCCs derived from cUC-iPSCs and cPBMC-iPSCs could be maintained over repeated passages and differentiated into iMSCs. High magnification images are shown within each picture. NCCs derived from CDF-iPSCs did not proliferate and differentiated into neuron-like cells with round cell bodies and elongated axon-like structures. Scale bars = 100  $\mu$ m. (B) The cell morphologies of PRIME-iMSCs derived from three different cell lines. The origin of PRIME-iMSCs is shown on the left side of the pictures: canine embryonic fibroblast-derived iPSCs (CEF-iPSCs), cUC-iPSCs, and cPBMC-iPSCs. These maintained their proliferation activities and bipolar or multipolar morphologies even after 11 passages. Scale bars = 100  $\mu$ m.

One possible explanation for the low *CD105* expression in PRIME-iMSCs could be the use of serum-free culture medium, which has been reported to decrease *CD105* expression in human MSCs [31,32]. Both flow cytometry and qPCR also showed that *CD90*

expression in PRIME-iMSCs was lower than in Ad-MSCs. However, PRIME-iMSCs derived from cUC-iPSCs displayed an increased ratio of *CD90* positive cells at latter passages, though the underlying mechanism remains unknown. Previous studies have suggested

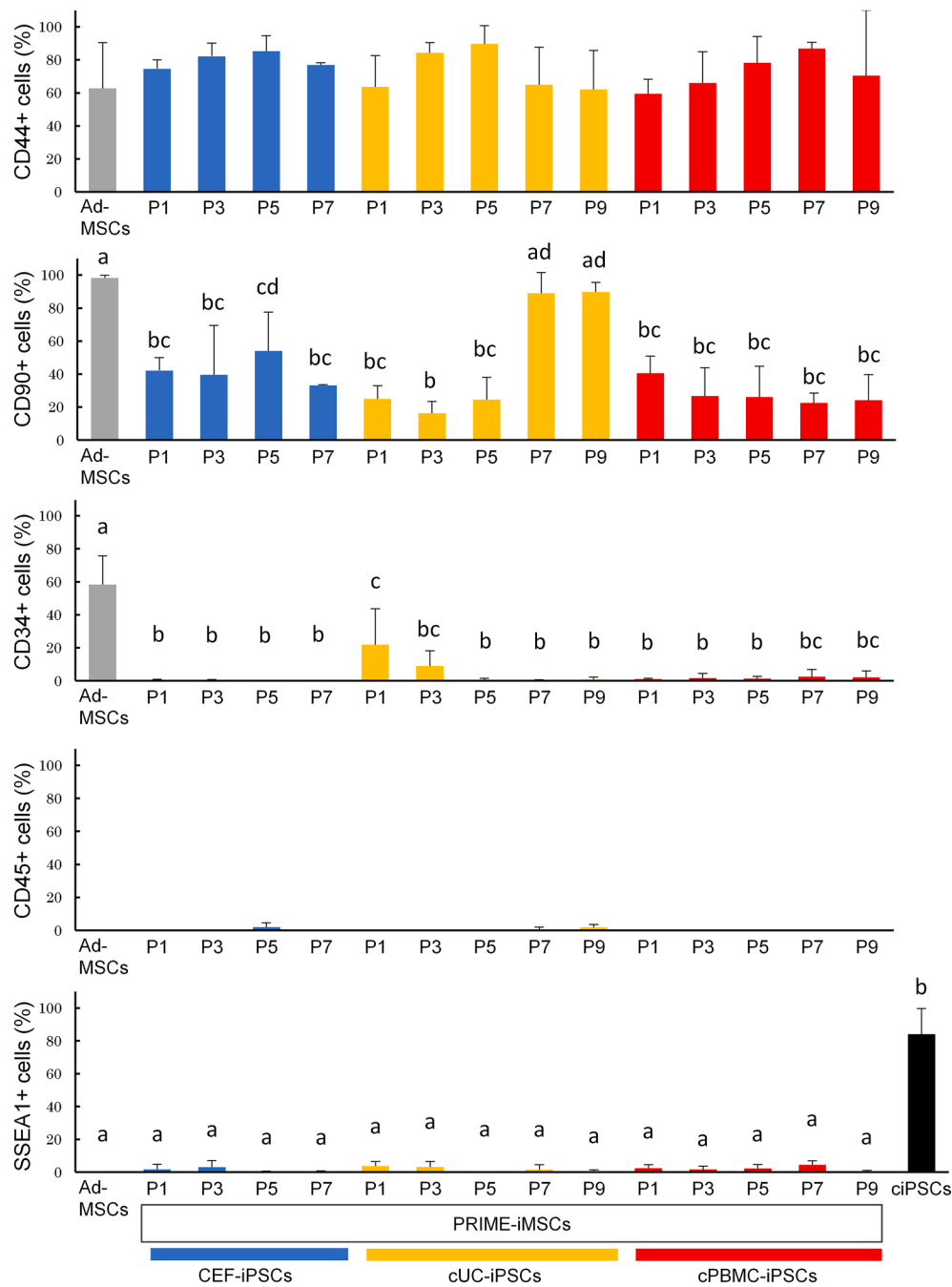


**Fig. 5.** Flow cytometry analysis for mesenchymal stem cell (MSC) negative and positive markers. CD44, CD90, CD34, CD45, and SSEA1 were used as MSC-positive and -negative markers, respectively. Adipose-derived MSCs (Ad-MSCs) and ciPSCs (for SSEA1) were used as controls (gray or black bars). Induced pluripotent stem cell (iPSC)-derived MSCs (iMSCs) were obtained using the neural crest cell (NCC) + PRIME protocol (PRIME-iMSCs). PRIME-iMSCs were generated from three canine iPSC lines: canine embryonic fibroblast (CEF)-derived iPSCs (CEF-iPSCs; blue bars), canine urine-derived cell (cUC)-derived iPSCs (cUC-iPSCs; yellow bars), and canine peripheral blood mononuclear cell (cPBMc)-derived iPSCs (cPBMc-iPSCs; red bars). Flow cytometry analysis was performed on PRIME-iMSCs at each passage number. Each experiment was performed three times as biological replicates. Data are shown as the mean  $\pm$  standard deviation ( $n = 3$ ). Within the graph, means marked with different letters (a, b, c, and d) are significantly different ( $P < 0.05$ ).

that CD90 expression is more variable than CD44 expression in canine MSCs [33,34]. Reduced CD90 expressions in human MSCs have reported to correlate with an increased differentiation capacity into tri-lineages [35], or a loss of immunosuppressive effect [36]. To our knowledge, no study has yet examined the role of CD90 in canine MSCs. Further study will be needed to understand the CD90 functions in canine iMSCs, and additional strategies, such as cell sorting, may be required to obtain more purified and homogeneous population of iMSCs from ciPSCs.

Although three ciPSC lines were induced to iMSCs, CDF-iPSCs failed to differentiate into PRIME-iMSCs, which could be attributed to the inability of CDF-iPSCs cultured in NCC to maintain their progenitor or stem cell properties. Human iPSC lines also exhibit considerable variation in their differentiation capacity, which can be attributed to epigenetic memory inherited from somatic cells or de novo variations during cell reprogramming and extended culture [19]. Although there is no solid evidence supporting inherent variations in ciPSCs, it is plausible that such variations exist. This



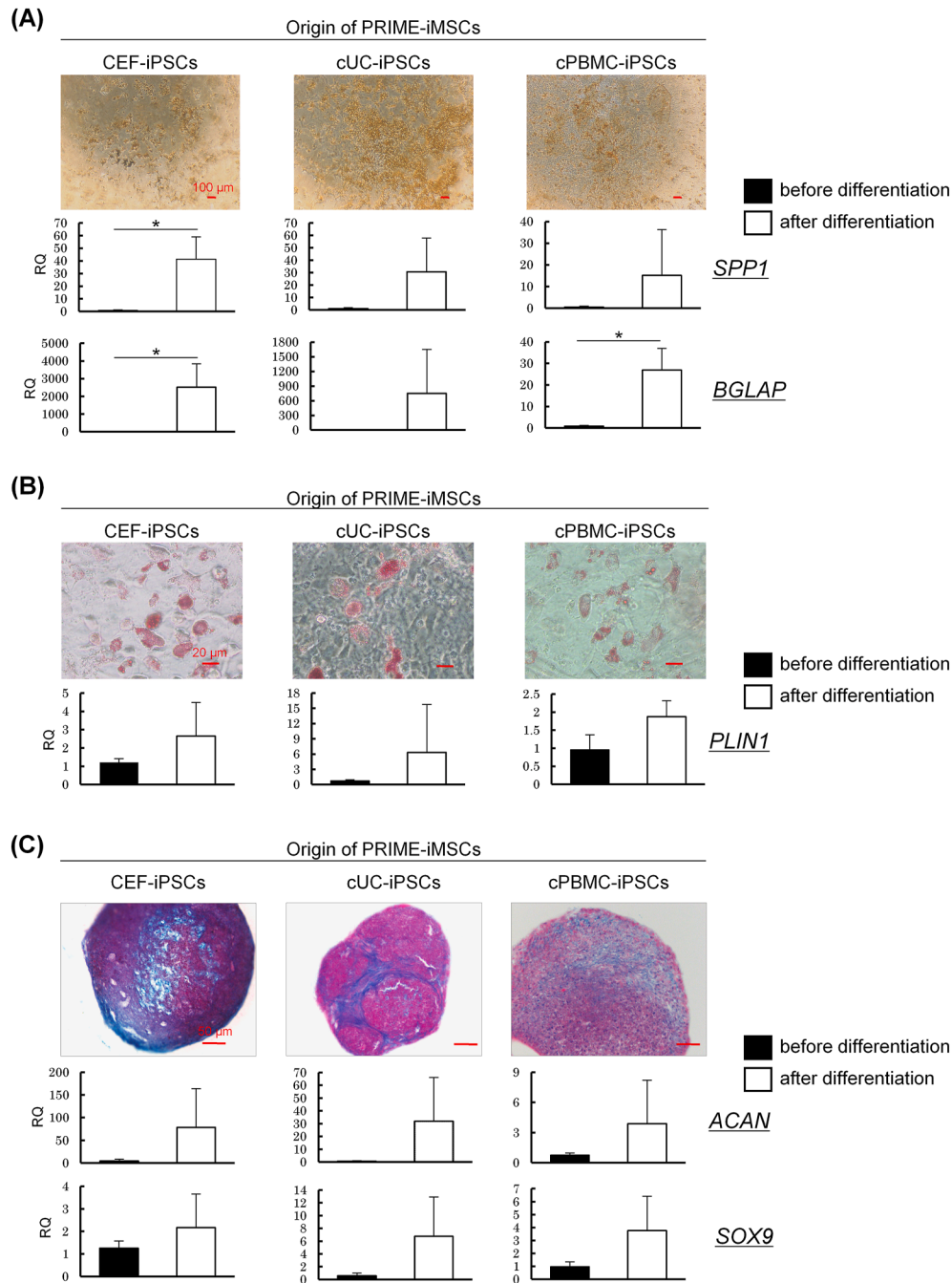


**Fig. 6.** Tri-lineage differentiation ability of induced pluripotent stem cell (iPSC)-derived mesenchymal stem cells (iMSCs) obtained using the neural crest cell (NCC) + PRIME protocol. iMSCs were obtained from canine embryonic fibroblast (CEF)-derived iPSCs (CEFi-iPSCs), canine urine-derived cell (cUC)-derived iPSCs (cUC-iPSCs), and canine peripheral blood mononuclear cell (cPBMC)-derived iPSCs (cPBMC-iPSCs) using the NCC + PRIME protocol. The origin of PRIME-iMSCs is represented on the upper side of the pictures. (A) Von Kossa staining after osteoblast induction. Von Kossa staining identified hydroxyapatite crystals in the extracellular matrix of differentiated cells. Scale bar = 100  $\mu$ m. qPCR for osteogenic markers, *SPP1* and *BGLAP*, were shown below the staining. Black bars and white bars represent iMSCs before and after differentiation. Data are presented as relative quantification (RQ) for iMSCs before differentiation and as the mean  $\pm$  standard deviation (n = 3). \*p < 0.05. (B) Oil Red O staining after adipocyte differentiation. The cells formed Oil Red O-positive lipid vacuoles in the cytoplasm. Scale bar = 20  $\mu$ m. qPCR for adipogenic marker, *PLIN1*, was shown below the staining. Black bars and white bars represent iMSCs before and after differentiation. Data are presented as RQ for iMSCs before differentiation and as the mean  $\pm$  standard deviation (n = 3). (C) Images of Alcian blue staining after chondrocyte induction. The iMSCs from all iPSC lines formed spheres and exhibited Alcian blue-positive proteoglycan production. Nuclei were stained red using nuclear fast red stain. Scale bar = 50  $\mu$ m. qPCR for chondrogenic markers, *ACAN* and *SOX9*, were shown below the picture. Black bars and white bars represent iMSCs before and after differentiation. Data are presented as RQ for iMSCs before differentiation and as the mean  $\pm$  standard deviation (n = 3).

hypothesis is supported by the observed differences in iMSC induction kinetics among different ciPSC sources, which are thought to be caused by variations in ciPSC characteristics [20] like with human iPSCs [19].

Cell therapy utilizing donor-derived MSCs has inherent limitations such as limited cell supply and variations arising from the donor's characteristics (such as age or sex), passage number, and original tissues of the MSCs [37–39]. Our study suggests that the

use of ciPSC-derived iMSCs offers a solution by providing a permanent and renewable source of MSCs. Furthermore, our study also suggests that differentiation kinetics and iMSC quality vary depending on the origin of ciPSC lines. Consequently, although we could not assess the immunosuppressive effect, the selection of ciPSC lines will be crucial in generating high-quality iMSCs suitable for cell therapy. Our findings have the potential to significantly contribute to the development of veterinary regenerative medicine.

## 5. Conclusions

Our study compared the induction methods of iMSCs from ciPSCs using either LPM or NCCs and demonstrated that the NCC + PRIME protocol resulted in the generation of more proliferative iMSCs with a higher expression of MSC markers. We observed differences in the differentiation kinetics of ciPSCs derived from the different somatic cell types and in the characteristics of iMSCs from different ciPSC lines. Although further investigations are necessary to evaluate the relationship between ciPSC lines as the origin of iMSCs, the expression of iMSC markers, and their functions including immunosuppressive effect, our findings provide valuable insights into the application of ciPSCs and iMSCs in the field of veterinary regenerative medicine.

## Declaration of competing interest

The authors declare that they have no conflicts of interest.

## Acknowledgments

This work was supported by JSPS KAKENHI (grant numbers JP18K19273, JP18H02349, JP19J22851, 20H03156, and 22H02525). We would like to thank Editage ([www.editage.com](http://www.editage.com)) for the English language editing.

## Appendix A. Supplementary data

Supplementary data to this article can be found online at <https://doi.org/10.1016/j.reth.2025.05.008>.

## References

- [1] Dominici M, Le Blanc K, Mueller I, Slaper-Cortenbach I, Marini FC, Krause DS, et al. Minimal criteria for defining multipotent mesenchymal stromal cells. The International Society for Cellular Therapy position statement. *Cytotherapy* 2006;8:315–7. <https://doi.org/10.1080/14653240600855905>.
- [2] Viswanathan S, Shi Y, Galièpeau J, Krampera M, Leblanc K, Martin I, et al. Mesenchymal stem versus stromal cells: international society for cell & gene therapy (ISCT®) mesenchymal stromal cell committee position statement on nomenclature. *Cytotherapy* 2019;21:1019–24. <https://doi.org/10.1016/j.jcyt.2019.08.002>.
- [3] Rodríguez-Fuentes DE, Fernández-Garza LE, Samia-Meza JA, Barrera-Barrera SA, Caplan AI, Barrera-Saldaña HA. Mesenchymal stem cells current clinical applications: a systematic review. *Arch Med Res* 2021;52:93–101. <https://doi.org/10.1016/j.arcmed.2020.08.006>.
- [4] Russell KA, Chow NHC, Dukoff D, Gibson TWG, La Marre J, Betts DH, et al. Characterization and immunomodulatory effects of canine adipose tissue- and bone marrow-derived mesenchymal stromal cells. *PLoS One* 2016;11. <https://doi.org/10.1371/JOURNAL.PONE.0167442>.
- [5] Song WJ, Li Q, Ryu MO, Ahn JO, Bhang DH, Jung YC, et al. TSG-6 released from intraperitoneally injected canine adipose tissue-derived mesenchymal stem cells ameliorate inflammatory bowel disease by inducing M2 macrophage switch in mice. *Stem Cell Res Ther* 2018;9. <https://doi.org/10.1186/s13287-018-0841-1>.
- [6] Chow L, Johnson V, Coy J, Regan D, Dow S. Mechanisms of immune suppression utilized by canine adipose and bone marrow-derived mesenchymal stem cells. *Stem Cells Dev* 2017;26:374–89. <https://doi.org/10.1089/SCD.2016.0207>.
- [7] Dias IE, Pinto PO, Barros LC, Viegas CA, Dias IR, Carvalho PP. Mesenchymal stem cells therapy in companion animals: useful for immune-mediated diseases? *BMC Vet Res* 2019;15. <https://doi.org/10.1186/s12917-019-2087-2>.
- [8] Kim HJ, Park J-S. Usage of human mesenchymal stem cells in cell-based therapy: advantages and disadvantages. *Dev Reprod* 2017;21:1–10. <https://doi.org/10.12717/DR.2017.21.1.001>.
- [9] Guercio A, Bella S Di, Casella S, Marco P Di, Russo C, Piccione G. Canine mesenchymal stem cells (MSCs): characterization in relation to donor age and adipose tissue-harvesting site. *Cell Biol Int* 2013;37:789–98. <https://doi.org/10.1002/CBIN.10090>.
- [10] Turinetto V, Vitale E, Giachino C. Senescence in human mesenchymal stem cells: functional changes and implications in stem cell-based therapy. *Int J Mol Sci* 2016;17. <https://doi.org/10.3390/IJMS17071164>.
- [11] Kretlow JD, Jin YQ, Liu W, Zhang WJ, Hong TH, Zhou G, et al. Donor age and cell passage affects differentiation potential of murine bone marrow-derived stem cells. *BMC Cell Biol* 2008;9. <https://doi.org/10.1186/1471-2121-9-60>.
- [12] Bloor AJC, Patel A, Griffin JE, Gillette MH, Radia R, Yeung DT, et al. Production, safety and efficacy of iPSC-derived mesenchymal stromal cells in acute steroid-resistant graft versus host disease: a phase I, multicenter, open-label, dose-escalation study. *Nat Med* 2020;26:1720–5. <https://doi.org/10.1038/s41591-020-1050-X>.
- [13] Jung Y, Bauer G, Nolte JA. Concise review: induced pluripotent stem cell-derived mesenchymal stem cells: progress toward safe clinical products. *Stem Cell* 2012;30:42–7. <https://doi.org/10.1002/STEM.727>.
- [14] Zhao C, Ikeya M. Generation and applications of induced pluripotent stem cell-derived mesenchymal stem cells. *Stem Cells Int* 2018;2018. <https://doi.org/10.1155/2018/9601623>.
- [15] de Matos BM, Robert AW, Stimamiglio MA, Correa A. Pluripotent-derived mesenchymal stem/stromal cells: an overview of the derivation protocol efficacies and the differences among the derived cells. *Stem Cell Rev Rep* 2022;18:94–125. <https://doi.org/10.1007/s12015-021-10258-Z>.
- [16] Eto S, Goto M, Soga M, Kaneko Y, Uehara Y, Mizuta H, et al. Mesenchymal stem cells derived from human iPSCs via mesoderm and neuroepithelium have different features and therapeutic potentials. *PLoS One* 2018;13. <https://doi.org/10.1371/JOURNAL.PONE.0200790>.
- [17] Chow L, Johnson V, Regan D, Wheat W, Webb S, Koch P, et al. Safety and immune regulatory properties of canine induced pluripotent stem cell-derived mesenchymal stem cells. *Stem Cell Res* 2017;25:221–32. <https://doi.org/10.1016/j.scr.2017.11.010>.
- [18] Whitworth DJ, Frith JE, Ovchinnikov DA, Cooper-White JJ, Wolvetang EJ. Derivation of mesenchymal stromal cells from canine induced pluripotent stem cells by inhibition of the TGF $\beta$ /activin signaling pathway. *Stem Cells Dev* 2014;23:3021–33. <https://doi.org/10.1089/SCD.2013.0634>.
- [19] Liang G, Zhang Y. Genetic and epigenetic variations in iPSCs: potential causes and implications for application. *Cell Stem Cell* 2013;13:149–59. <https://doi.org/10.1016/j.stem.2013.07.001>.
- [20] Tsukamoto M, Kimura K, Yoshida T, Tanaka M, Kuwamura M, Ayabe T, et al. Generation of canine induced pluripotent stem cells under feeder-free conditions using Sendai virus vector encoding six canine reprogramming factors. *Stem Cell Rep* 2024;19:141–57. <https://doi.org/10.1016/j.stemcr.2023.11.010>.
- [21] Kimura K, Tsukamoto M, Yoshida T, Tanaka M, Kuwamura M, Ohtaka M, et al. Canine induced pluripotent stem cell maintenance under feeder-free and chemically-defined conditions. *Mol Reprod Dev* 2021;88:395–404. <https://doi.org/10.1002/MRD.23478>.
- [22] Chen YS, Pelekanos RA, Ellis RL, Horne R, Wolvetang EJ, Fisk NM. Small molecule mesenchymal induction of human induced pluripotent stem cells to generate mesenchymal stem/stromal cells. *Stem Cells Transl Med* 2012;1:83–95. <https://doi.org/10.5966/SCTM.2011-0022>.
- [23] Mitsuzawa S, Zhao C, Ikeguchi R, Aoyama T, Kamiya D, Ando M, et al. Pro-angiogenic scaffold-free Bio three-dimensional conduit developed from human induced pluripotent stem cell-derived mesenchymal stem cells promotes peripheral nerve regeneration. *Sci Rep* 2020;10. <https://doi.org/10.1038/s41598-020-68745-1>.
- [24] Malagola E, Teunissen M, Van Der Laan LJW, Verstegen MMA, Schotanus BA, Van Steenbeek FG, et al. Characterization and comparison of canine multipotent stromal cells derived from liver and bone marrow. *Stem Cells Dev* 2016;25:139–50. <https://doi.org/10.1089/SCD.2015.0125>.
- [25] Lian Q, Zhang Y, Zhang J, Zhang HK, Wu X, Zhang Y, et al. Functional mesenchymal stem cells derived from human induced pluripotent stem cells attenuate limb ischemia in mice. *Circulation* 2010;121:1113–23. <https://doi.org/10.1161/CIRCULATIONAHA.109.898312>.
- [26] Lee JY, Kang MH, Jang JE, Lee JE, Yang Y, Choi JY, et al. Comparative analysis of mesenchymal stem cells cultivated in serum free media. *Sci Rep* 2022;12. <https://doi.org/10.1038/s41598-022-12467-z>.
- [27] Liu Z, Screven R, Boxer L, Myers MJ, Devireddy LR. Characterization of canine adipose-derived mesenchymal stromal/stem cells in serum-free medium. *Tissue Eng Part C Methods* 2018;24:399–411. <https://doi.org/10.1089/TEN.TEC.2017.0409>.
- [28] Li E, Zhang Z, Jiang B, Yan L, Park JW, Xu RH. Generation of mesenchymal stem cells from human embryonic stem cells in a complete serum-free condition. *Int J Biol Sci* 2018;14:1901–9. <https://doi.org/10.7150/IJBS.25306>.
- [29] Guest DJ, Dudhia J, Smith RKW, Roberts SJ, Conzemius M, Innes JF, et al. Position statement: minimal criteria for reporting veterinary and animal medicine research for mesenchymal stromal/stem cells in orthopedic applications. *Front Vet Sci* 2022;9. <https://doi.org/10.3389/FVETS.2022.817041>.

- [30] Bearden RN, Huggins SS, Cummings KJ, Smith R, Gregory CA, Saunders WB. In-vitro characterization of canine multipotent stromal cells isolated from synovium, bone marrow, and adipose tissue: a donor-matched comparative study. *Stem Cell Res Ther* 2017;8. <https://doi.org/10.1186/S13287-017-0639-6>.
- [31] Wang D, Liu N, Xie Y, Song B, Kong S, Sun X. Different culture method changing CD105 expression in amniotic fluid MSCs without affecting differentiation ability or immune function. *J Cell Mol Med* 2020;24:4212–22. <https://doi.org/10.1111/JCMM.15081>.
- [32] Mark P, Kleinsorge M, Gaebel R, Lux CA, Toelk A, Pittermann E, et al. Human mesenchymal stem cells display reduced expression of CD105 after culture in serum-free medium. *Stem Cells Int* 2013;2013. <https://doi.org/10.1155/2013/698076>.
- [33] Takemitsu H, Zhao D, Yamamoto I, Harada Y, Michishita M, Arai T. Comparison of bone marrow and adipose tissue-derived canine mesenchymal stem cells. *BMC Vet Res* 2012;8. <https://doi.org/10.1186/1746-6148-8-150>.
- [34] Screven R, Kenyon E, Myers MJ, Yancy HF, Skasko M, Boxer L, et al. Immunophenotype and gene expression profile of mesenchymal stem cells derived from canine adipose tissue and bone marrow. *Vet Immunol Immunopathol* 2014;161:21–31. <https://doi.org/10.1016/J.VETIMM.2014.06.002>.
- [35] Moraes DA, Sibov TT, Pavon LF, Alvim PQ, Bonadio RS, Da Silva JR, et al. A reduction in CD90 (THY-1) expression results in increased differentiation of mesenchymal stromal cells. *Stem Cell Res Ther* 2016;7. <https://doi.org/10.1186/S13287-016-0359-3>.
- [36] Campioni D, Rizzo R, Stignani M, Melchiorri L, Ferrari L, Moretti S, et al. A decreased positivity for CD90 on human mesenchymal stromal cells (MSCs) is associated with a loss of immunosuppressive activity by MSCs. *Cytometry B Clin Cytom* 2009;76:225–30. <https://doi.org/10.1002/CYTO.B.20461>.
- [37] Siegel G, Kluba T, Hermanutz-Klein U, Bieback K, Northoff H, Schäfer R. Phenotype, donor age and gender affect function of human bone marrow-derived mesenchymal stromal cells. *BMC Med* 2013;11. <https://doi.org/10.1186/1741-7015-11-146>.
- [38] Rojewski MT, Weber BM, Schrezenmeier H. Phenotypic characterization of mesenchymal stem cells from various tissues. *Transfus Med Hemother* 2008;35:168–84. <https://doi.org/10.1159/000129013>.
- [39] Zaim M, Karaman S, Cetin G, Isik S. Donor age and long-term culture affect differentiation and proliferation of human bone marrow mesenchymal stem cells. *Ann Hematol* 2012;91:1175–86. <https://doi.org/10.1007/S00277-012-1438-X>.